Centrum voor Wiskunde en Informatica
REPORT*RAPPORT*

Analysis of Oil Lens Removal by Extraction through a Seepage Face

M.I.J. van Dijke, S.E.A.T.M. van der Zee

Modelling, Analysis and Simulation (MAS)

MAS-R9725 September 30, 1997

Report MAS-R9725
ISSN 1386-3703

CWI
P.O. Box 94079
1090 GB Amsterdam
The Netherlands

Analysis of Oil Lens Removal by Extraction through a Seepage Face

M.I.J. van Dijke
CWI
P.O. Box 94079, 1090 GB Amsterdam, The Netherlands

S.E.A.T.M. van der Zee
Department of Soil Science and Plant Nutrition, Wageningen Agricultural University
P.O. Box 8005, 6700 EC Wageningen, The Netherlands

ABSTRACT
Removal of LNAPL (oil) from an aquifer is described using a multi-phase flow model. At the well boundary seepage face conditions are imposed. These conditions are implemented in a numerical model and withdrawal in a two-dimensional domain is simulated for two different geometries of the oil lens and for varied values of the physical parameters. Assuming vertical equilibrium, the oil flow equation is reduced by vertical integration. The well boundary condition is approximated by imposing zero oil lens thickness. Similarity solutions of the reduced equations for the two geometries show good agreement with the numerical results in most cases.

1991 Mathematics Subject Classification: 35R35, 65M06, 76S05, 76T05
Keywords and Phrases: multi-phase flow, LNAPL lens, removal, seepage face, vertical equilibrium, similarity solutions, numerical simulations
Note: Work carried out under project MAS1.3 "Partial Differential Equations in Porous Media Research".

1. Introduction

Spills of hydrocarbons have caused contamination of numerous aquifers. Nonaqeous phase liquids, such as gasoline, that are less dense than water (henceforth called oil for brevity), may accumulate as a lens at the phreatic water surface. To remediate the contaminated aquifers, the bulk of oil in the lens is usually first removed by pump and treat methods, after which the remaining (trapped) oil is removed by other techniques, such as air sparging or bioremediation.

Pumping is commonly done through vertically drilled extraction filters or in horizontal ditches in case of shallow lenses. If the extraction well or ditch is partially filled with fluid, two fluid phases may seep out of the soil above the well fluid level, similar to water seepage in the dam problem [6, 12]. Multi-phase seepage is a complicated process, since the nonwetting phase may seep out at virtually zero saturations [1, 27].

During pumping often a drawdown of the water table is created to facilitate oil flow towards the extraction well. Such a local lowering of the water table may smear out the oil and increase both the oil-invaded region and the amount of trapped oil. For this reason the drawdown of the water table is preferably kept small. If the slope of the water table is small, the lens may be at vertical flow equilibrium, except close to the pumping well or ditch. At vertical equilibrium pressure distributions are hydrostatic and therefore the vertical dimension of the multi-phase flow problem can be eliminated by vertical integration of variables. In that situation only the oil flow equation needs to be considered [7, 21, 23, 25].

Corapcioglu e.a. [11] modeled an axisymmetric two-pump recovery system, in which the lower well was assumed to create a drawdown of the water table and the upper well was assumed to extract free oil at a constant rate. They used a sharp-interface approach and assumed that the well was located

within the oil lens at any time, which may only be realistic during the early stages of pumping when the oil layer is relatively thick. After linearizing equations analytical solutions were obtained.

Huyakorn e.a. and Wu e.a. [16, 26] numerically investigated withdrawal of an oil lens in a three-dimensional domain assuming vertical flow equilibrium. In [16] withdrawal wells were assumed to operate under prescribed volumetric extraction rates, where the separate water and oil extraction rates were determined by the phase mobilities. In [26] the well bore pressure and the productivity index for a local grid block were computed as in the oil reservoir engineering literature, see e.g. [13], to determine the separate water and oil extraction rates. Both studies were restricted to the part of the oil lens where only water and oil were present, thus neglecting the three-phase zone.

Wu e.a. [27] discussed numerical implementation of seepage boundary conditions, also for three-phase flow. Although at seepage boundaries the well pressure is known, they imposed sink terms for water and oil similar to the well conditions of [26] with a large artificial productivity index.

In this study we present a model for the behavior of an oil lens on the water table in a two-dimensional domain for two lens geometries, where withdrawal occurs through a well with constant fluid level. To treat the corresponding multi-phase seepage face conditions, we impose the so called Signorini conditions. Numerically, we compared implementation of these conditions as sink terms according to [27] to a more direct implementation. For the situation in which the well fluid level is equal to the phreatic water surface in the soil, we perform several numerical computations and give an indication of their accuracy, especially near the seepage boundary.

As numerical models still require large computation times and are not always able to handle the boundary conditions accurately, approximate analytical solutions can be very helpful. We use the vertical equilibrium assumption of capillarity-gravity-segregated flow to reduce the multi-phase flow problem to a single equation for oil flow [7, 25]. In the vertically integrated problem for the layer thickness we approximate the well boundary condition by taking lens thickness equal to zero. Similar problems for water outflow from an aquifer, with sharp interfaces, were studied by Boussinesq [6] and by Barenblatt [4] who derived analytical solutions. We use the generalizations of these analytical solutions that account for capillary forces, to describe oil lens extraction with possible incorporation of oil entrapment by water. In Appendix 3 we show that a similar analytical solution can be obtained for oil removal in a semi-infinite three-dimensional domain.

The analytical solutions are compared with the numerical results. We indicate in which cases the analytical solutions with the approximate well condition appropriately approximate the solutions of the nonreduced flow model.

2. Model

We model withdrawal of an oil lens in a two-dimensional domain $0 < X < L$, $-\infty < Z < \infty$, with $L > 0$, and a well at $X = 0$. Two important situations that are different with respect to the horizontal extension of the domain, are considered. The first concerns a horizontally bounded domain as shown in Figure 1.a, i.e. $L < \infty$, which reflects either the left half of a symmetric domain with a second well at $X = 2\,L$ or a situation with a vertical impervious boundary at $X = L$. The second concerns a domain, that is unbounded to the right, as shown in Figure 1.b, i.e. $L = \infty$, where the oil lens is bounded by $X = X_l$ and can spread out in horizontal direction.

We use for both water (w) and oil (o) the mass balance equations

$$\phi\,\frac{\partial\,S_j}{\partial\,T} + \frac{\partial\,U_j}{\partial\,X} + \frac{\partial\,V_j}{\partial\,Z} = 0, \quad j = w, o \tag{2.1}$$

and Darcy's Law

$$U_j = -\frac{K\,k_{rj}}{\mu_j}\,\frac{\partial\,P_j}{\partial\,X} \tag{2.2}$$

$$V_j = -\frac{K\,k_{rj}}{\mu_j}\,\left(\frac{\partial\,P_j}{\partial\,Z} + \rho_j\,g\right), \quad j = w, o, \tag{2.3}$$

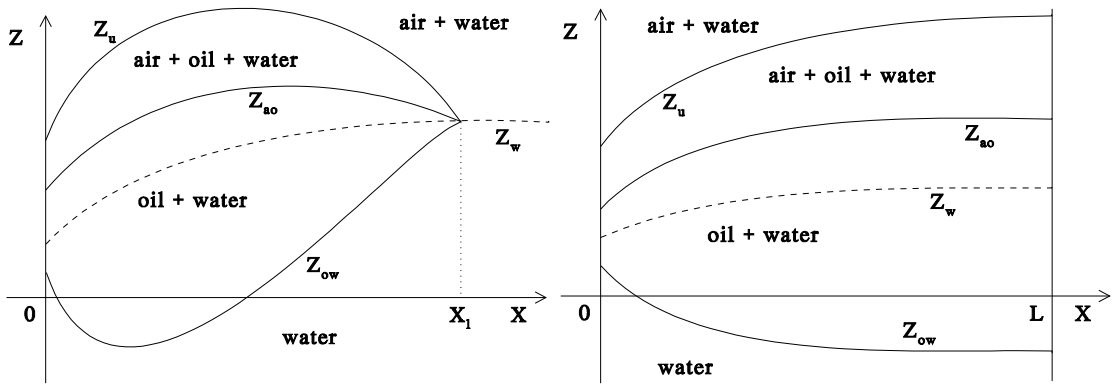

Figure 1: Geometry of an oil lens in a domain that is bounded to the right (a) and that is unbounded to the right (b).

where T is time, X and Z are the horizontal and vertical coordinates respectively, S_j is effective phase saturation, U_j and V_j are phase horizontal and vertical flow velocities respectively, P_j is phase pressure, ρ_j phase density, k_{rj} phase relative permeability, μ_j phase viscosity, ϕ porosity, K absolute permeability and g gravitation. We assume that the soil is homogeneous and isotropic, that both fluids are incompressible and that air is present with saturation S_a and constant pressure ($P_a = 0$). According to [22] we define the total fluid saturation S_t, trapped oil saturation S_{ot}, free oil saturation S_{of}, apparent water saturation S_{wa}, oil-water capillary pressure P_{ow} and air-oil capillary pressure P_{ao}, which satisfy the constitutive relations

$$\begin{aligned} S_w + S_o &= S_t \\ S_t + S_a &= 1 \\ S_w + S_{ot} &= S_{wa} \\ S_{of} + S_{ot} &= S_o \\ P_{ow} &= P_o - P_w \\ P_{ao} &= -P_o. \end{aligned}$$

For the retention functions we use

$$S_{wa} = \begin{cases} 1 & \text{if } P_w > 0 \text{ and } P_o < P_w \\ \left(1 + \left(\dfrac{\alpha_{ow}}{\rho_w g} P_{ow}\right)^n\right)^{\frac{1}{n}-1} & \text{if } \begin{cases} 0 < P_w < P_o \text{ or} \\ P_w < 0 \text{ and } P_o > \dfrac{1}{\beta_{ao}} P_w \end{cases} \\ \left(1 + \left(\dfrac{-\alpha}{\rho_w g} P_w\right)^n\right)^{\frac{1}{n}-1} & \text{if } P_o < \dfrac{1}{\beta_{ao}} P_w < 0 \end{cases} \tag{2.4}$$

$$S_t = \begin{cases} 1 & \text{if } P_o > 0 \text{ or } P_w > 0 \\ \left(1 + \left(\dfrac{\alpha_{ao}}{\rho_w g} P_{ao}\right)^n\right)^{\frac{1}{n}-1} & \text{if } \dfrac{1}{\beta_{ao}} P_w < P_o < 0 \\ S_{wa} & \text{if } P_o < \dfrac{1}{\beta_{ao}} P_w < 0, \end{cases} \tag{2.5}$$

where $\alpha > 0$ and $n > 1$ are soil parameters. Furthermore, $\alpha_{ow} = \alpha\,\beta_{ow}$ and $\alpha_{ao} = \alpha\,\beta_{ao}$, where β_{ow} and β_{ao} are the ratios of the oil-water and the air-oil to the air-water surface tensions, with $\dfrac{1}{\beta_{ow}} + \dfrac{1}{\beta_{ao}} = 1$. Relative permeabilities satisfy [19]

$$k_{rw} = S_w{}^{\frac{1}{2}} \left(1 - \left(1 - S_w^{\frac{n}{n-1}}\right)^{1-\frac{1}{n}}\right)^2 \tag{2.6}$$

$$k_{ro} = (S_t - S_{wa})^{\frac{1}{2}} \left(\left(1 - S_{wa}^{\frac{n}{n-1}}\right)^{1-\frac{1}{n}} - \left(1 - S_t^{\frac{n}{n-1}}\right)^{1-\frac{1}{n}}\right)^2. \tag{2.7}$$

At locations where oil has been present we model oil entrapment by the linear relation [25]

$$S_{ot} = \begin{cases} \theta\,\left(S_{wa} - S_w^{min}\right) & \text{if } S_{wa} > S_w^{min} \\ 0 & \text{if } S_{wa} = S_w^{min}, \end{cases} \tag{2.8}$$

where the minimum water saturation S_w^{min} is given by

$$S_w^{min}(X, Z, T) = \min_{T' \le T} S_w(X, Z, T'). \tag{2.9}$$

The constant $\theta \in [0, 1]$ is the maximum trapped oil saturation, which is obtained when $S_w^{min} = 0$ and $S_{wa} = 1$.

Equations (2.1), (2.2) and (2.3) are solved for time $T > 0$ in the domain of Figure 1. The free oil is confined to two layers [23]. Between the levels $Z = Z_u$ and $Z = Z_{ao}$ water, (free) oil and air are present, whereas between the levels $Z = Z_{ao}$ and $Z = Z_{ow}$ only water and (free) oil are present. At the level $Z = Z_w$ we have $P_w = 0$, which corresponds outside the oil lens to the phreatic surface. For $L = \infty$ the levels Z_u, Z_{ao} and Z_{ow} coincide for $X = X_l$ at $Z = Z_w$. Hence, $Z_{ow}(X, T)$, $Z_{ao}(X, T)$, $Z_u(X, T)$ are defined by

$$\begin{aligned} &S_t = 1, \quad S_{of} = 0 \quad \text{if } Z < Z_{ow} \\ &S_t = 1, \quad S_{of} > 0 \quad \text{if } Z_{ow} < Z < Z_{ao} \\ &S_t < 1, \quad S_{of} > 0 \quad \text{if } Z_{ao} < Z < Z_u \\ &S_t < 1, \quad S_{of} = 0 \quad \text{if } Z > Z_u, \end{aligned}$$

In terms of capillary pressures these levels are given by

$$P_{ow}(Z_{ow}) = 0, \quad P_{ao}(Z_{ao}) = 0, \quad \frac{\beta_{ao}}{\beta_{ow}} P_{ao}(Z_u) = P_{ow}(Z_u). \tag{2.10}$$

In the well at the left side of the boundary $X = 0$ the fluid level is fixed at $Z = 0$. We impose well conditions, which may include seepage of oil at the entire boundary $X = 0$ and seepage of water for $Z > 0$. At seepage boundaries a certain phase can only flow out, in which case its pressure is equal to the pressure outside the porous medium [10, 12]. Hence, similar to water seepage in the dam problem [6, 12], we impose the Signorini conditions [2, 14] for multi-phase seepage

$$\begin{aligned} &P_w \le P_{out}, \quad U_w \le 0, \quad (P_w - P_{out})\,U_w = 0 \quad \text{for } X = 0,\ Z > 0 \\ &P_o \le P_{out}, \quad U_o \le 0, \quad (P_o - P_{out})\,U_o = 0 \quad \text{for } X = 0,\ -\infty < Z < \infty, \end{aligned} \tag{2.11}$$

and also

$$P_w = P_{out} \qquad \text{for } X = 0,\ Z \le 0, \tag{2.12}$$

where

$$P_{out}(Z) = \begin{cases} 0 & \text{for } Z > 0 \\ -\rho_w\, g\, Z & \text{for } Z \le 0. \end{cases} \tag{2.13}$$

For $L < \infty$ we impose additionally no-flow conditions at $X = L$, i.e. $U_j = 0$ for $j = w, o$.
At $T = 0$ we take initial pressure distributions

$$\left.\begin{array}{rcl} P_w\,(X,Z,0) & = & P_{w,i}\,(X,Z) \\ P_o\,(X,Z,0) & = & P_{o,i}\,(X,Z) \end{array}\right\} \quad \text{for } 0 < X < L,\ -\infty < Z < \infty, \tag{2.14}$$

such that oil has nonzero saturation $S_{o,i}$ in a lens with the finite horizontal extension $X_l \leq L$, which has prescribed volume

$$\mathcal{V}_0 = \phi \int_{-\infty}^{\infty} \int_0^{\infty} S_{o,i}\, dX\, dZ = \phi \int_{Z_{ow}}^{Z_u} \int_0^{X_l} \left(S_t\,(P_{o,i}) - S_{wa}\,(P_{w,i}, P_{o,i})\right)\, dX\, dZ. \tag{2.15}$$

If $L < \infty$ we identify $X_l \equiv L$. At $T = 0$ no oil is trapped.

We define characteristic horizontal lengthscales according to

$$X_c = \left\{ \begin{array}{ll} L & \text{for } L < \infty \\ \alpha_{ow}\, \mathcal{V}_0 & \text{for } L = \infty \end{array}\right. \tag{2.16}$$

and a characteristic vertical lengthscale, velocity, pressure and time according to

$$Z_c = \frac{1}{\alpha_{ow}}, \quad U_c = \frac{K\, \rho_o\, g}{\mu_o}, \quad P_c = \frac{\rho_o\, g}{\alpha_{ow}}, \quad T_c = \frac{X_c}{U_c} \tag{2.17}$$

This leads to the dimensionless variables

$$u_j = \frac{U_j}{U_c},\ v_j = \frac{V_j}{U_c},\ p_j = \frac{P_j}{P_c},\ x = \frac{X}{X_c},\ z = \frac{Z}{Z_c},\ t = \frac{T}{T_c}, \quad j = w, o. \tag{2.18}$$

Similarly, P_{out}, $P_{w,i}$, $P_{o,i}$, X_l, Z_w, Z_{ow}, Z_{ao} and Z_u become dimensionless by scaling with P_c, X_c and Z_c.

Combining equations (2.1), (2.2) and (2.3) into two Richards equations the resulting problem is ($j = w, o$)

$$\phi\, \frac{\partial\, S_j}{\partial\, t} - \frac{\mu_o}{\mu_j} \left(\frac{Z_c}{X_c}\, \frac{\partial}{\partial\, x} \left(k_{rj}\, \frac{\partial\, p_j}{\partial\, x} \right) + \frac{X_c}{Z_c}\, \frac{\partial}{\partial\, z} \left(k_{rj} \left(\frac{\partial\, p_j}{\partial\, z} + \frac{\rho_j}{\rho_o} \right) \right) \right) = 0 \tag{2.19}$$

for $x > 0,\ -\infty < z < \infty,\ t > 0$. The boundary conditions become

$$\begin{array}{ll} p_j \leq 0, \quad u_j \leq 0, \quad p_j\, u_j = 0 & \text{for } x = 0,\ z > 0 \\ \left.\begin{array}{l} p_w = -\dfrac{\rho_w}{\rho_o}\, z \\ p_o \leq -\dfrac{\rho_w}{\rho_o}\, z,\ u_o \leq 0,\ \left(p_o + \dfrac{\rho_w}{\rho_o}\, z \right)\, u_o = 0 \end{array}\right\} & \text{for } x = 0,\ z \leq 0 \end{array} \tag{2.20}$$

and additionally for the bounded domain $u_j = 0$ for $x = 1,\ -\infty < z < \infty$. The initial conditions are

$$\left.\begin{array}{rcl} p_w\,(x,z,0) & = & p_{w,i}\,(x,z) \\ p_o\,(x,z,0) & = & p_{o,i}\,(x,z) \end{array}\right\} \quad \text{for } x > 0,\ -\infty < z < \infty, \tag{2.21}$$

with

$$\phi \int_{z_{ow}}^{z_u} \int_0^{x_l} \left(S_t\,(p_{o,i}) - S_{wa}\,(p_{w,i}, p_{o,i})\right)\, dx\, dz = \upsilon_0, \tag{2.22}$$

where $\upsilon_0 = \dfrac{\mathcal{V}_0}{X_c\, Z_c}$.

3. Numerical results

3.1 Numerical model

We simulated the withdrawal of an oil lens with the numerical model of [24, 25], which we adapted for the seepage face boundary conditions. In this model equations (2.1), (2.2) and (2.3) are combined into the mixed form of the Richards equation [9, 17] for both water and oil. Computations were done in non-transformed physical variables. The flow domain was discretized by linear triangular finite elements. Time discretization was fully implicit. The resulting algebraic equations were solved by the modified Picard method [9], that gave good mass balances. Convergence was obtained for the Picard iterations by adjusting the time steps. The initial time step was 0.10 hours and the maximum allowable time step 50 hours.

Some soil and fluid parameters were not varied:

$$\begin{array}{llll} K_{abs} = 7.09 \cdot 10^{-12}\ \mathrm{m}^2, & \phi = 0.400, & & \\ \mu_w = 1.00 \cdot 10^{-3}\ \mathrm{Pa\,s}, & \rho_w = 1.00 \cdot 10^3 & \mathrm{kg\,m^{-3}}, & \\ \mu_o = 5.00 \cdot 10^{-4}\ \mathrm{Pa\,s}, & g = 9.80 & \mathrm{m\,s^{-2}}. & \end{array}$$

We varied the parameters L, $\mathcal{V}_0$, n, α, β_{ow}, ρ_o and θ as summarized in Table 1. Additionally, the maximum computed times T_e and the characteristic lengths and times are listed.

Table 1: Parameters and characteristic lengths and times that were used in the computations. Case 1 reflects the simulation with different treatments of the seepage face conditions, case 2 the simulation with grid refinements, case 3-10 the simulations on the unbounded domain and case 11-18 the simulations on the bounded domain.

case	L (m)	$\mathcal{V}_0$ (m^3)	n	α (m^{-1})	β_{ow}	ρ_o (10^3 kg m^{-3})	θ	T_e (10^3 h)	Z_c (m)	X_c (m)	T_c (h)
1	∞	0.200	3.0	1.00	2.25	0.700	0.0	1.00	0.444	0.450	1.285
2	10.0	1.00	3.0	1.00	2.25	0.700	0.0	10.0	0.444	10.0	28.56
3	∞	1.00	3.0	1.00	2.25	0.700	0.0	50.0	0.444	2.25	6.425
4	∞	1.00	2.0	1.00	2.25	0.700	0.0	50.0	0.444	2.25	6.425
5	∞	1.00	5.0	1.00	2.25	0.700	0.0	50.0	0.444	2.25	6.425
6	∞	1.00	3.0	2.00	2.25	0.700	0.0	50.0	0.222	4.50	12.85
7	∞	1.00	3.0	1.00	1.80	0.700	0.0	50.0	0.556	1.80	5.140
8	∞	1.00	3.0	1.00	2.25	0.850	0.0	50.0	0.444	2.25	5.291
9	∞	1.00	3.0	1.00	2.25	0.700	0.30	50.0	0.444	2.25	6.425
10	∞	1.00	3.0	1.00	2.25	0.700	0.45	50.0	0.444	2.25	6.425
11	10.0	1.00	3.0	1.00	2.25	0.700	0.0	60.0	0.444	10.0	28.56
12	10.0	1.00	2.0	1.00	2.25	0.700	0.0	30.0	0.444	10.0	28.56
13	10.0	1.00	5.0	1.00	2.25	0.700	0.0	100	0.444	10.0	28.56
14	10.0	1.00	3.0	2.00	2.25	0.700	0.0	100	0.222	10.0	28.56
15	10.0	1.00	3.0	1.00	1.80	0.700	0.0	60.0	0.556	10.0	28.56
16	10.0	1.00	3.0	1.00	2.25	0.850	0.0	60.0	0.444	10.0	23.52
17	10.0	1.00	3.0	1.00	2.25	0.700	0.30	60.0	0.444	10.0	28.56
18	10.0	1.00	3.0	1.00	2.25	0.700	0.45	60.0	0.444	10.0	28.56

3.2 Treatment of seepage face conditions

Condition (2.11) requires that at nodes of the seepage boundary either a velocity (no-flow) or a pressure is prescribed. We compare two approaches to dealing with this condition numerically.

In an attempt to model all types of boundary conditions by source / sink terms, it has been proposed [27] to treat this variational condition by imposing at every phase j seepage node the sink

term (in physical dimensions)

$$U_j = -\chi \frac{K\, k_{rj}}{\mu_j} \max\left(0, P_j - P_{out}\right), \tag{3.1}$$

where χ is a large number. In this condition the pressure gradient of the horizontal flow velocity (2.2) is replaced by the product $\chi \cdot (P_j - P_{out})$ and consequently a large value of χ represents a fine mesh in the X-direction. The underlying concept is that the flow velocity U_j remains non-zero, even at nodes where the oil relative permeability approaches zero, which happens if both fluids are flowing, or if the pressure difference $P_j - P_{out}$ goes to zero. During every time step condition (3.1) is evaluated implicitly, such that after convergence the correct outflow velocity and pressure P_j are approximated. For a flowing phase the latter becomes almost equal to P_{out}. Unfortunately, if χ is large, the convergence requires large numbers of iterations.

Alternatively, the well-conditions can be treated straightforwardly by imposing at every seepage node

$$\begin{cases} P_j = P_{out} & \text{if } U_j < 0 \\ U_j = 0 & \text{if } P_j < P_{out}. \end{cases} \tag{3.2}$$

Hence, if the pressure is imposed exactly equal to the outside pressure, the flow velocity is computed as usual from equation (2.2) using the pressure gradient over the grid element adjacent to the boundary and the element averaged oil relative permeability. For a sufficiently fine X-discretization, we obtain accurate results with a limited number of iterations. As the stiffness matrix with its modifications for Dirichlet conditions is not changed during a time step, we evaluate condition (3.2) at the end of each time step, where the automatic time stepping guarantees sufficient accuracy.

To compare the effect of the 'iterative' condition (3.1) and the 'direct' condition (3.2), we simulated flow with the set of parameters of case 1 of Table 1. A domain of 16.5 m wide and 1.5 m high was used, with uniform Z-discretization (19 nodes). For the X-discretization (41 nodes) element widths increased from 0.068 m to 0.679 m for increasing X. The top and bottom boundaries were taken impermeable to both phases and the right boundary was impermeable to oil. The water level at the well boundary at the left side ($X = 0$), was taken at 0.5 m above the bottom of the domain. At the right boundary, water pressures were taken hydrostatic with $P_w = 0$ again at 0.5 m above the bottom, yielding an essentially horizontal water table. At $T = 0$ h we imposed hydraulic heads ($H_{j,i} = \dfrac{P_{j,i}}{\rho_w\, g} + \dfrac{\rho_j}{\rho_w}\, Z$) for each phase, given by

$$\begin{aligned} H_{w,i} &= \quad 0.0 \text{ m} \quad \text{for } 0.0 < X < 16.5 \text{ m},\ -0.5 < Z < 1.0 \text{ m} \\ H_{o,i} &= \begin{cases} \quad 0.0 \text{ m} & \text{for } 0.0 < X < 0.1, \text{ and } 4.0 < X < 16.5 \text{ m},\ -0.5 < Z < 1.0 \text{ m} \\ 0.172 \text{ m} & \text{for } 0.1 < X < 4.0 \text{ m},\ -0.5 < Z < 1.0 \text{ m}, \end{cases} \end{aligned} \tag{3.3}$$

such that 0.200 m^3 oil was present in the domain. This simulation reflects withdrawal in an unbounded domain ($L = \infty$) in the sense of Figure 1.a. Multi-phase flow during 1000 h was computed, where the well conditions were treated either by condition (3.1) with $\chi = 100$ m^{-1} and $\chi = 1000$ m^{-1} respectively, or by condition (3.2). In Figure 2 we compare the results in terms of the vertically integrated (free) oil saturations $w_f = \phi \int S_{of}\, dz$ at three times and in terms of the oil volume in the domain $v = \phi \int\int S_{of}\, dx\, dz$. As oil flows out only through the well boundary, the oil volume can be obtained from the cumulative oil outflow rate: $\int_0^t \int_z u_o(0, \zeta, \tau)\, d\zeta\, d\tau = 1 - v$. Figure 2 shows that as χ increases, the 'iterative' solutions appear to converge to the solution obtained with the 'direct' condition.

Figure 2.c shows the oil pressure distribution at the well boundary. At about $z = 0.35$ the well condition switches from the zero pressure to the no-flow condition, whereas the oil pressure is hydrostatic for $z > 0.35$. This level marks the top of the oil seepage face. For $z < 0$ the oil pressure is equal to the water pressure and hence the oil saturation is zero, but oil flows out at those nodes where oil is present

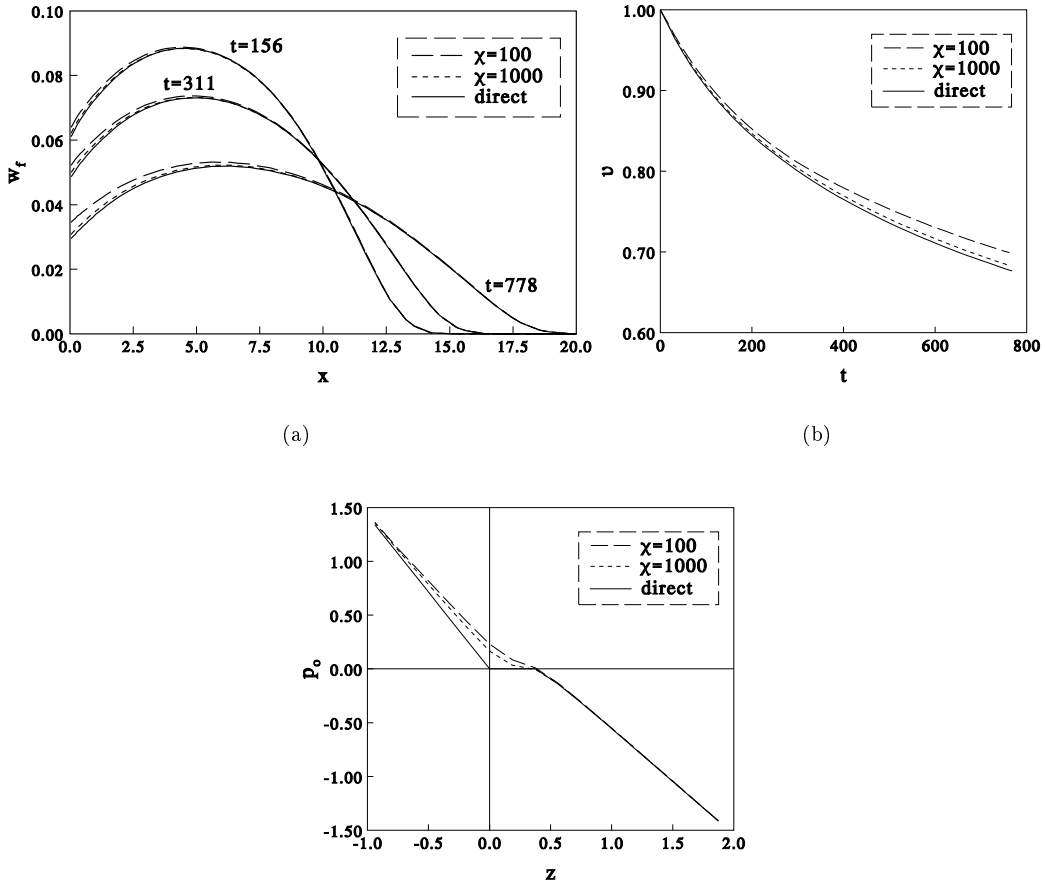

Figure 2: Comparison of seepage face treatment (case 1) by the 'iterative' condition (with $\chi = 100$, $\chi = 1000$) and the 'direct' condition in terms of vertically integrated oil saturations w_f as a function of x (a), oil volume in the domain v as a function of t (b) and oil pressure distribution p_o at the well boundary as a function of z at $t = 156$ (c).

inside the domain. We observe that the 'iterative' condition yields a smoothed approximation of the correct oil pressure p_o at the well boundary. For the larger value of χ the approximation is slightly better in agreement with the exact condition. However, the number of (Picard) iterations and time steps needed for convergence becomes very large: the present simulation with $\chi = 100$ took about 6 h and with $\chi = 1000$ about 45 h, whereas the simulation with the 'direct' condition required only 20 min. Hence, at least for this type of computations the 'direct' approach is preferable.

3.3 Grid refinements

Especially near the part of the well boundary where oil flows out, large pressure gradients occur and the effects of discretization may be substantial. To investigate this, we performed a series of simulations in which we refined both the X-grid and the Z-grid near the well boundary. A domain of 10.0 m wide and 2.5 m high was used. For every simulation the X-grid between 1.0 and 10.0 m had 15 elements, whose widths increased from 0.351 to 0.849 m, and the Z-grid between 0.5 and 2.0 m had 15 elements of uniform height. The X-discretization between 0.0 and 1.0 m and the Z-discretization between -0.5 and 0.5 m were varied as follows:

grid x1 : 3 elements, width increasing from 0.111 to 0.556 m,
grid x2 : 6 elements, width increasing from 0.028 to 0.306 m,
grid x3 : 12 elements, width increasing from 0.007 to 0.160 m,
grid z1 : 5 elements, height 0.20 m,
grid z2 : 10 elements, height 0.10 m,
grid z3 : 20 elements, height 0.05 m.

We considered the combinations (x1,z3), (x2,z3), (x3,z3), (x3,z1) and (x3,z2) and simulated flow with the set of parameters of case 2 of Table 1. The top, bottom and right boundaries were taken impermeable to both phases, which reflects withdrawal from an essentially bounded domain, see Figure 1.b. The water level at the well boundary was taken at 0.5 m above the bottom of the domain. At $T = 0$ h we imposed for each phase hydraulic heads

$$\begin{array}{ll} H_{w,i} = 0.0 \text{ m} & \text{for } 0.0 < X < 10.0 \text{ m},\ -0.5 < Z < 2.0 \text{ m} \\ H_{o,i} = 0.215 \text{ m} & \text{for } 0.0 < X < 10.0 \text{ m},\ -0.5 < Z < 2.0 \text{ m} \end{array} \tag{3.4}$$

such that 1.0 m^3 oil was present in the domain. Multi-phase flow during 10000 h was simulated.

In Figure 3 the solutions corresponding to the refinements are presented in terms of the vertically integrated oil saturations at three times. The solutions corresponding to the x-grid refinement seem to converge, but since the differences between solutions corresponding to the z-grid refinement do not uniformly decrease, the dependence on the z-grid near the well boundary is less straightforward.

The situation near the well boundary is illustrated by Figure 4. In Figure 4.a oil pressures are given for X between 0.0 and 0.5 m and Z between -0.5 and 0.5 m in dimensionless variables at $T = 10000$ h. Observe that roughly above $z = 0.30$ oil pressures are negative and nearly hydrostatically distributed and no oil flows out. Below $z = -0.80$ oil pressures are equal to the hydrostatic water pressures, which means that oil is neither present nor does it flow out. Between $z = -0.80$ and $z = 0.30$ oil flows out and large oil pressure gradients occur, which cause numerical difficulties.

Figure 4.b shows the horizontal water u_w and oil u_o flow velocities at the well boundary between $z = -0.60$ and $z = 0.60$ at 5 different times. For the present situation with no decline of the water table throughout the domain only water inflow occurred below the well water level. Oil flowed out mainly above this water level with velocities, that were much larger than the water inflow velocities. Between $t = 210$ and $t = 350$ the maximum level where oil flowed out, i.e. the top of the oil seepage face, decreased from $z = 0.3375$ to $z = 0.225$, which are the positions of two horizontal gridlines. As oil outflow is maximum just below and vanishes abruptly at the top of the seepage face, this may be another source of numerical difficulties.

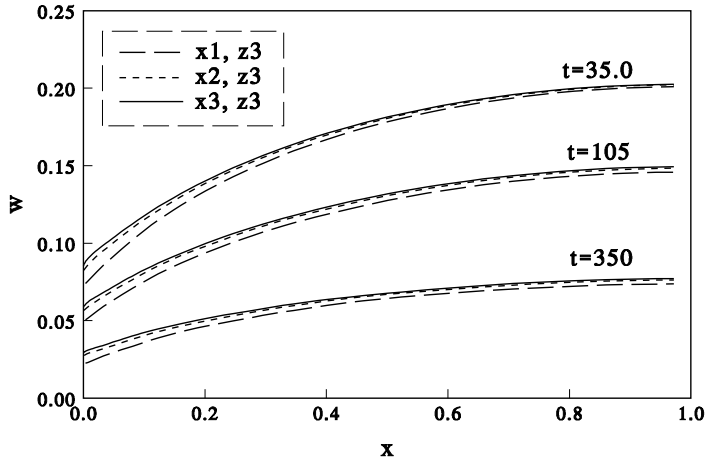

(a)

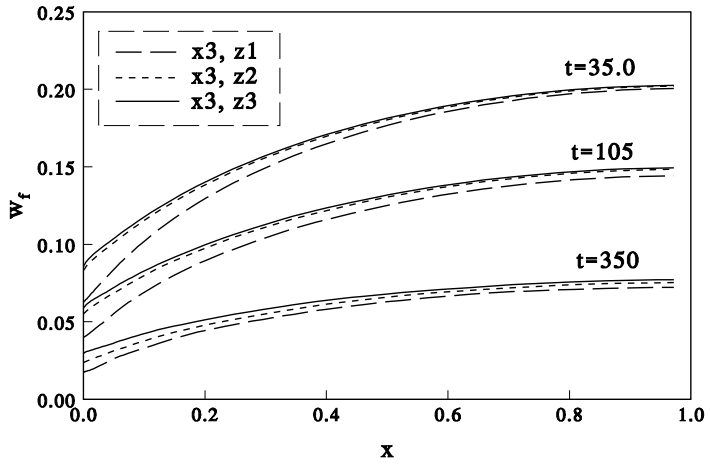

(b)

Figure 3: Vertically integrated oil saturations w_f (case 2) as a function of x for refinement of x-grid near the well boundary (a) and for refinement of z-grid near the well boundary (b).

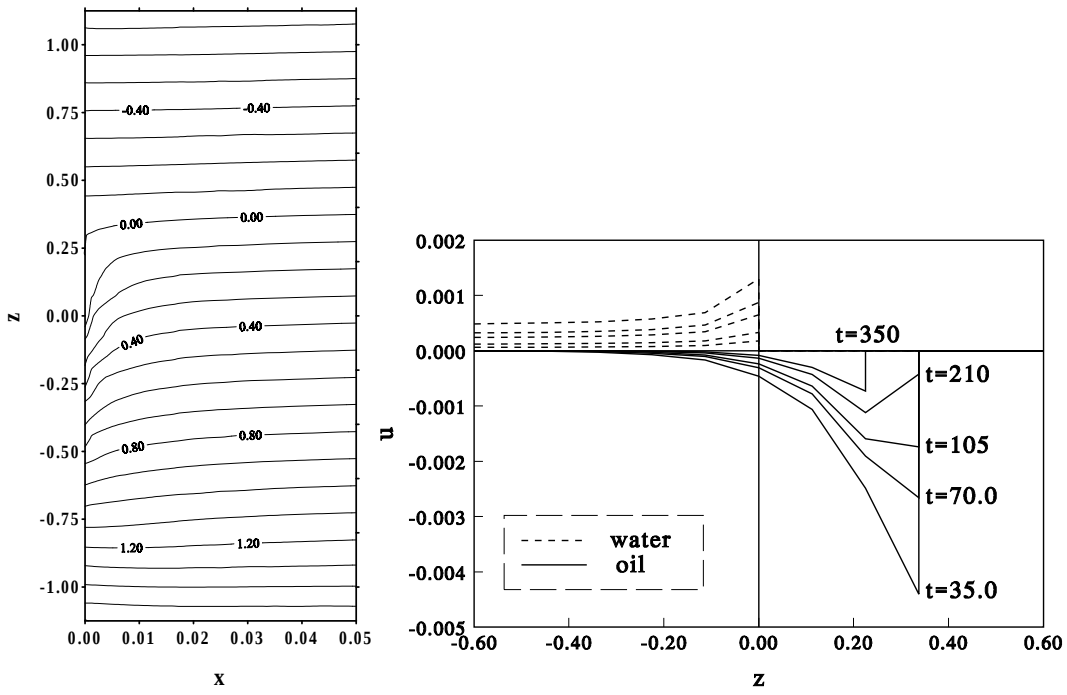

(a) (b)

Figure 4: Oil pressure contourlines in the neighbourhood of the well boundary $t = 350$ (a) and water and oil flow velocities at the well boundary at several times (b) for the grid refinement (x3,z3) (case 2).

3.4 Sensitivity analysis

With condition (3.2) and grid refinement (x3,z3) near the seepage boundary, we performed a series of simulations in which we varied parameters as shown in Table 1, with case 3 as a reference case for the unbounded domain simulations 3 to 10 and case 11 for the bounded domain simulations 11 to 18. For the unbounded domain the X-grid (from 1 to 55 m) consisted of 42 elements, whose widths increased from 0.356 to 2.215 m, and the Z-grid for the entire domain was the same as near the well boundary, with 15 elements of uniform height between 0.5 and 2.0 m, which yielded 1980 nodepoints in total. Initially, we imposed water hydraulic heads $H_{w,i} = 0.0$ m throughout the entire domain and oil hydraulic heads such that 1.0 m^3 oil was present in the domain (e.g. for case 3 $H_{o,i} = 0.215$ m for $0.0 < X < 9.6$ m, $H_{o,i} = 0.107$ m for $9.6 < X < 12$ m and $H_{o,i} = 0.0$ m for $X > 12$ m). These computations took typically 16 h on a HP 9000 735/125 workstation. For the bounded domain the discretization (1008 nodepoints) and initial conditions were taken the same as in case 2. The corresponding computation times were typically about 3 h.

For the unbounded domain cases the profiles of w_f were similar to those shown in Figure 2.a, whereas for the bounded domain cases the profiles looked like those of Figure 3. The varied parameters n, α, β_{ow} and ρ_o most likely affect the thickness of the oil layers and thus the seepage flow rate.

In Figure 5 we present the removal rates, i.e. the evolution of v. We observe that removal happens much slower in the unbounded domain (Figure 5.a) than in the bounded domain (Figure 5.b). As expected the van Genuchten parameter n largely affects the removal rate, in the sense that large values of n correspond with slow removal (cases 5 and 13). The effects of changing α, β_{ow} and ρ_o (cases 6, 7, 8, 14, 15 and 16) are not very large. The larger value of the parameter α (cases 6 and 14) slighty fastens the removal, which is contrary to the effect that α has on other processes like oil lens redistribution, see e.g. [25]. The coincidence of cases 7 and 8 happened by chance. As expected also the trapping parameter θ is important, especially because a large amount of oil cannot be removed at all.

In Figure 6 we present for the unbounded domain cases the first moment in x-direction of the vertically integrated free oil saturations $M_1 = \phi \int x\, w_f \, dx\, dz$. These moments itself have no important physical meaning, but we observe that for most cases they became almost constant after a very short time, which we will come back to in Section 4.3. Only for a large value of n (case 5) and for the entrapment cases 9 and 10 the moment did not become constant.

4. Analytical approximations

4.1 Reduced equations

To obtain analytical approximations for the decay of the oil lens at an essentially horizontal water table, we assume that vertical oil velocities can be neglected. According to [6] a necessary condition for this vertical flow equilibrium is that the horizontal extension of the lens is much larger than its vertical extension, say $X_l/(Z_u - Z_{ow}) \gg 1$. Then, the vertical capillary and the gravitational forces balance and capillary pressures are hydrostatically distributed. Furthermore, if additionally the oil saturations, and thus the oil mobilities, are much smaller than the water saturations and mobilities, we may assume that the water pressures are hydrostatically distributed with reference level $p_w = 0$ at $z = 0$, and thus water and oil flow are segregated [25]. The numerical results indicate that the vertical equilibrium assumption is justified shortly after the start of the flow process everywhere in the lens away from the well boundary, see also [25]. The vertical pressure distributions are given by

$$p_w = -\frac{\rho_w}{\rho_o} z \qquad \text{for } -\infty < z < \infty \tag{4.1}$$

$$p_o = z_{ao} - z \qquad \text{for } z_{ow} < z < z_u. \tag{4.2}$$

According to definition (2.10) we may relate the separating levels in the oil lens by

$$z_{ow} = -\frac{\rho_o}{\Delta\rho} z_{ao}, \quad z_u = \frac{\beta_{ow}}{1-D} z_{ao} \quad \text{with } D = \frac{\beta_{ow}\,\Delta\rho}{\beta_{ao}\,\rho_o} \tag{4.3}$$

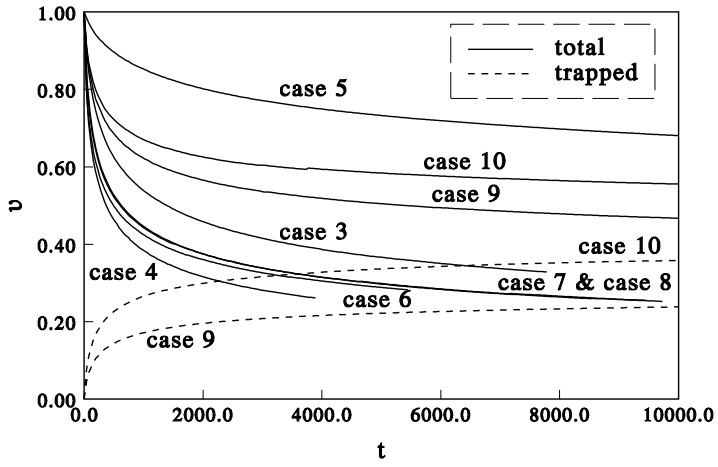

(a)

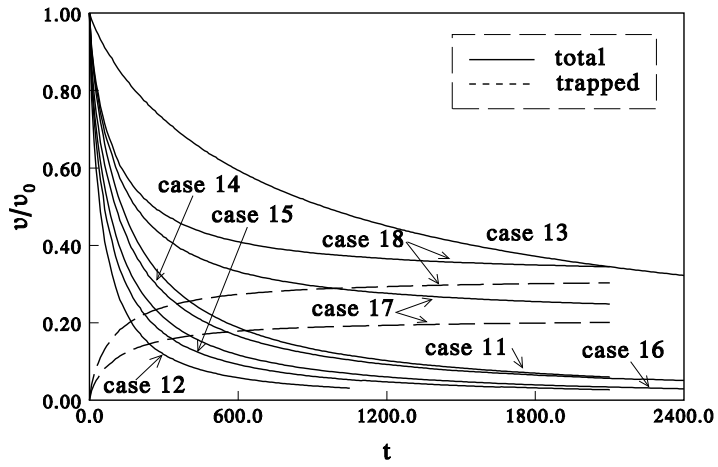

(b)

Figure 5: Oil volumes as a function of time for the unbounded domain (a) and for the bounded domain (relative to the initial volume) (b). For cases 9, 10, 17 and 18 also the trapped oil volumes are shown.

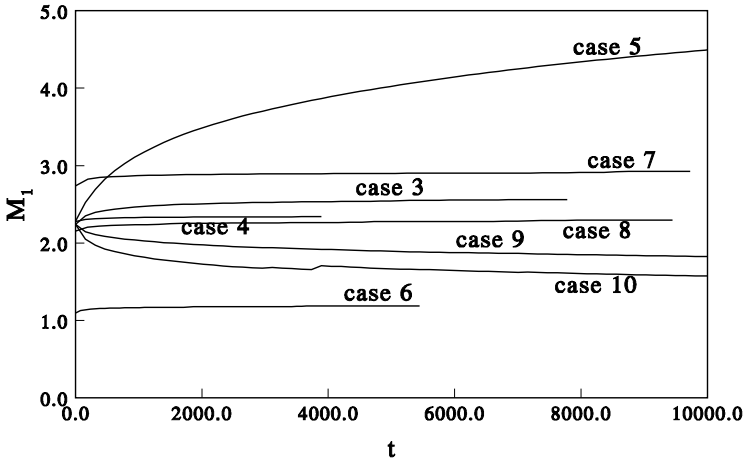

Figure 6: First moments of the vertically integrated free oil saturations as a function of time for the unbounded domain.

and $\Delta\rho = \rho_w - \rho_o$. To ensure that oil is confined to layers of finite thickness, we take $D < 1$ [8, 20]. Neglecting vertical velocities, equation (2.19) for oil

$$\phi \frac{\partial S_o}{\partial t} - \frac{Z_c}{X_c} \frac{\partial}{\partial x} \left(k_{rj} \frac{\partial z_{ao}}{\partial x} \right) = 0 \tag{4.4}$$

describes the entire flow process [7, 25].

Because vertical pressure distributions are hydrostatic, we further reduce equation (4.4) by vertical integration, which requires evaluation of

$$w_f = \phi \int_{z_{ow}}^{z_u} S_{of}\, dz = \phi \int_{z_{ow}}^{z_u} (S_t - S_{wa})\, dz \tag{4.5}$$

$$\bar{k} = \int_{z_{ow}}^{z_u} k_{ro}(S_{wa}, S_t)\, dz = \int_{z_{ow}}^{z_u} k_{ro}(S_{wa}, S_t)\, dz, \tag{4.6}$$

where $w_f(r,t)$ represents the free oil volume per unit lateral area and $\bar{k}(r,t)$ the vertically integrated relative permeability [7, 16, 23, 25, 26]. To rewrite equation (4.4) in terms of the variable w_f only, we approximate both $\bar{k}$ and z_{ao} by power law functions of w_f in Appendix 1. To achieve this, we approximate the retention functions (2.4) and (2.5) by power law functions, which is reasonable in case of vertical flow equilibrium [25]. We obtain

$$z_{ao} = \lambda_1\, w_f^{\frac{1}{n+1}} \quad \text{and} \quad \bar{k} = \lambda_2\, w_f^{\frac{5n-2}{2\,(n+1)}}, \tag{4.7}$$

where λ_1 and λ_2 are given by (A 16) and (A 17).

Additionally, we define $w_o(r,t)$ as the total oil volume per unit lateral area, $w_t(r,t)$ as the trapped oil volume, with $w_t = w_o - w_f$, and $w_m(r,t)$ as the maximum oil volume, i.e.

$$w_m(r,t) = \max_{t' \le t} w_f(r,t'). \tag{4.8}$$

The hydrostatic pressure assumption implies that for every lateral position the integrated apparent water saturation attains its minumum at the time w_f attains its maximum. Hence, the vertically

integrated trapping mechanism (2.8) is given by

$$w_t = \begin{cases} c_t\,(w_m - w_f) & \text{if } \dfrac{\partial\, w_f}{\partial\, t} \le 0 \\ 0 & \text{if } \dfrac{\partial\, w_f}{\partial\, t} > 0 \end{cases} \tag{4.9}$$

at every lateral position where w_f is positive, with $c_t = \dfrac{\rho_o}{\rho_w}\,\theta$ [25], see Appendix 1. Writing the vertically integrated time derivative of equation (4.4) as

$$\frac{\partial\, w_o}{\partial\, t} = \begin{cases} \dfrac{\partial\, w_f}{\partial\, t} & \text{if } \dfrac{\partial\, w_f}{\partial\, t} > 0 \\ \dfrac{\partial\, w_f}{\partial\, t}\,(1 - c_t) & \text{if } \dfrac{\partial\, w_f}{\partial\, t} \le 0, \end{cases} \tag{4.10}$$

we arrive at the nonlinear diffusion equation

$$F\,(\frac{\partial\, w_f}{\partial\, t}) = \gamma\,\frac{\partial}{\partial\, x}\,(w_f^m\,\frac{\partial\, w_f}{\partial\, x}) \quad \text{for } t > 0,\ 0 < x < x_l, \tag{4.11}$$

where

$$p = \frac{1}{1 - c_t}, \qquad p \ge 1 \tag{4.12}$$

$$\gamma = \frac{Z_c\, p\, \lambda_1\, \lambda_2}{X_c\,(n+1)} \tag{4.13}$$

$$m = \frac{3n-2}{2\,(n+1)}, \qquad \frac{1}{4} < m < \frac{3}{2} \tag{4.14}$$

and F is defined for argument y by

$$F(y) = \begin{cases} p\, y & \text{if } y > 0 \\ y & \text{if } y \le 0. \end{cases} \tag{4.15}$$

Observe that if entrapment is not included, $p = 1$ and $F(y) = y$ for all y, whereas for the bounded domain w_f is decreasing everywhere and simply yields $F(y) \equiv y$.

Near the well boundary oil pressures are not hydrostatically distributed and equation (4.11) is not valid. Therefore, it is not possible to relate w_f to the level z_{ao} (4.7) and to transform the well condition (2.20) into an appropriate condtion for w_f at the well boundary. However, we know that below the well water level oil saturations are zero and we assume that the part of the seepage boundary above the water level is small. Hence, we impose the Dirichlet condition

$$w_f\,(0, t) = 0 \tag{4.16}$$

and mention that for (4.16) the outflow rate $q(t) = -\gamma\, w_f^m\,\dfrac{\partial\, w_f}{\partial\, x}(0, t)$ is nonzero provided $\dfrac{\partial\, w_f}{\partial\, x}(0, t) = \infty$.

Furthermore, if $L < \infty$ we impose at the right boundary the no-flow condition

$$\frac{\partial\, w_f}{\partial\, x}\,(1, t) = 0. \tag{4.17}$$

The initial condition corresponding to (2.14) is

$$w_f\,(x, 0) = w_i(x), \tag{4.18}$$

where $w_i = \phi \int S_i \, dz$ is the initial oil volume per unit lateral area. According to condition (2.15) w_i satisfies

$$\int_0^{x_l} w_i \, (x) \, dr = v_0. \tag{4.19}$$

For $L = \infty$ we mention two important features of w_f which can be verified easily. The 'diffusion' coefficient w_f^m vanishes for $w_f = 0$, which implies that the free boundary x_l which separates the regions where $w_f > 0$ and $w_f = 0$, is at every time at finite distance from the z-axis. Considering that the speed s_l at which the free boundary moves is equal to the horizontal oil velocity at the free boundary, this speed is given by [4, 7]

$$s_l = \lim_{x \uparrow x_l} w_f^{m-1} \, \frac{\partial \, w_f}{\partial \, x}. \tag{4.20}$$

Furthermore, if $p = 1$ the first moment of w_f satisfies [4]

$$\int_0^{x_l} x \, w_f \, dx = \text{const.} \tag{4.21}$$

4.2 Analytical solutions

Equation (4.11) is the (modified) porous medium equation which admits similarity solutions of the form [3, 15]

$$w_{f\,a}(x, \bar{t}) = \bar{t}^{\,-\mu} \, h(x \, \bar{t}^{\,-\nu}), \tag{4.22}$$

with constant μ and ν. We have introduced $\bar{t} = \gamma \, (t - t_0)$ with t_0 representing the time at which the solution becomes singular.

For $L < \infty$, the solution of equation (4.11) is positive on the fixed region $[0, 1]$, which requires $\nu = 0$, and the transformation (4.22) is a simple separation of variables. Substitution of (4.22) with $\nu = 0$ into equation (4.11) yields $\mu = \dfrac{1}{m}$ and the ordinary differential equation

$$(h^{\,m} \, h')' = -\frac{h}{m} \qquad \text{for } 0 < \eta < 1 \tag{4.23}$$

for $h(\eta)$, with $\eta \equiv x$. To facilitate the computation of h, we apply the scaling

$$\tilde{h}(\xi) = C^{-\frac{2}{m}} \, h(C \, \xi), \quad \xi = \frac{\eta}{C}, \tag{4.24}$$

for any positive constant C [21, 25]. In this case we take $C = 1$, because the length of the domain is equal to 1 and $\tilde{h}$ is the solution of equation (4.23) on the domain $0 < \xi < 1$, where primes $'$ denote differentiation with respect to ξ.

Scaling of the boundary conditions (4.16) and (4.17) yields $\tilde{h}(0) = 0$ and $\tilde{h}\,'(1) = 0$. To derive the corresponding solution of equation (4.23), which was obtained by Boussinesq [6] for $m = 1$, we substitute $\tilde{y} = -\tilde{h}^{\,m} \, \tilde{h}\,'$, the transformed oil flux. The resulting equation for $\tilde{y}(\tilde{h})$ has the solution

$$\tilde{y}(\tilde{h}) = -\sqrt{\frac{2}{m \, (m+2)}} \sqrt{\tilde{h}^{m+2}(1) - \tilde{h}^{m+2}}. \tag{4.25}$$

Hence, we obtain implicitly for $\tilde{h}(\xi)$

$$\xi = \sqrt{\frac{m \, \tilde{h}^m(1)}{2 \, (m+2)}} \, B_{\left(\frac{\tilde{h}(\xi)}{\tilde{h}(1)}\right)^{m+2}} \left(\frac{m+1}{m+2}, \frac{1}{2} \right), \tag{4.26}$$

where

$$B_\zeta(a,b) = \int_0^\zeta \tau^{a-1}(1-\tau)^{b-1}\,d\tau, \tag{4.27}$$

is the incomplete B-function. Substitution of $\xi = 1$ into equation (4.26), yields the value of $\tilde{h}(1)$. Inserting $\tilde{h}(1)$ in (4.25) gives the flux $\tilde{y}(\tilde{h})$, in particular at $\xi = 0$.

For $L = \infty$, we write the similarity solution (4.22) for convenience as

$$w_{fa}(x,t) = \begin{cases} \bar{t}^{-\mu}\, h(x\,\nu^{\frac{1}{2}}\,\bar{t}^{-\nu}) & \text{for } 0 < x < A\,\nu^{-\frac{1}{2}}\,\bar{t}^{\nu} \\ 0 & \text{for } x \geq A\,\nu^{-\frac{1}{2}}\,\bar{t}^{\nu}, \end{cases} \tag{4.28}$$

where $A\,\nu^{-\frac{1}{2}}\,\bar{t}^{\nu}$, with positive A, represents the free boundary beyond which $w_{fa} = 0$. Substitution of (4.28) into equation (4.11) shows that the similarity profile $h(\eta)$, with variable $\eta = x\,\nu^{\frac{1}{2}}\,\bar{t}^{-\nu}$, satisfies the equation

$$(h^{\,m}\,h')' = F(-\eta\,h' - k\,h) \quad \text{for } 0 < \eta < A, \tag{4.29}$$

with $k = \dfrac{\mu}{\nu}$, and μ and ν satisfying

$$2\,\nu + m\,\mu - 1 = 0. \tag{4.30}$$

Observe that for the similarity solution (4.28) the moment $M_{k-1} = \int x^{k-1}\,w_f\,dx$ is time-independent [25], i.e.

$$M_{k-1,a} = \nu^{-\frac{1}{2}\,k} \int_0^A \eta^{k-1}\,h(\eta)\,d\eta, \tag{4.31}$$

which is a generalization of property (4.21).

After the scaling (4.24) with $C = A$, $\tilde{h}$ is the solution of equation (4.29) for $0 < \xi < 1$. Boundary condition (4.16) yields $\tilde{h}(0) = 0$ and at the free boundary we have $\tilde{h}(1) = 0$.

For $p = 1$ property (4.21) requires $k = 2$, i.e.

$$\mu = 2\,\nu = \frac{1}{m+1}, \tag{4.32}$$

and equation (4.29) has the explicit Dipole solution [5, 15]

$$\tilde{h}(\xi) = \left(\frac{m\,(m+1)}{m+2}\,(\xi^{\frac{m}{m+1}} - \xi^2)\right)^{\frac{1}{m}}. \tag{4.33}$$

The transformed oil flux $\tilde{y} = -\tilde{h}^{\,m}\,\tilde{h}'$ at $\xi = 0$ is given by

$$\tilde{y}(\xi = 0) = -\frac{1}{m+1}\left(\frac{m\,(m+1)}{m+2}\right)^{1+\frac{1}{m}}. \tag{4.34}$$

The first moment of $\tilde{h}$, which is the transformed version of the moment (4.31) for $k = 2$, i.e. $\int \xi\,\tilde{h}\,d\xi$, is given by

$$\tilde{M}_1 = \frac{m+1}{m+2}\left(\frac{m\,(m+1)}{m+2}\right)^{\frac{1}{m}} B\left(\frac{m+1}{m+2}+1, \frac{1}{m}+1\right), \tag{4.35}$$

where $B = B_1$ (4.27) is the B-function.

For $p > 1$ the trapping parameter k and the solution of equation (4.29) cannot be found exactly. Hence, we compute numerically the similarity profile and the value of k, see also [25], for which the procedure is described in Appendix 2. We obtain the trapping parameter k as a function of p, which is shown in Figure 7 for different m-values.

In Appendix 3 we show that a similarity solution similar to (4.28) can be obtained for oil removal in a semi-infinite three-dimensional domain.

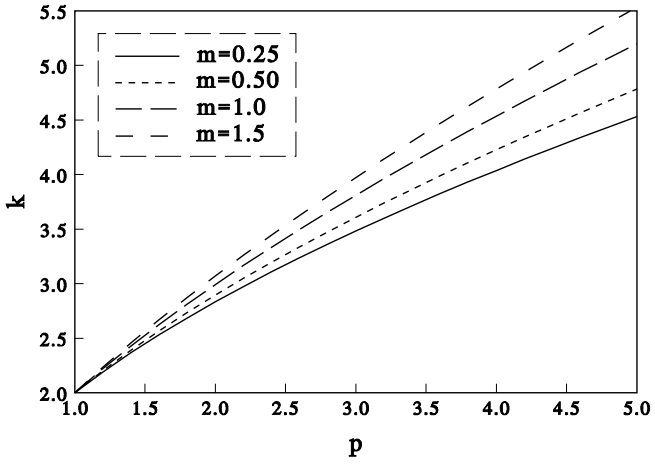

Figure 7: Parameter k as a function p for several values of m.

4.3 Agreement between numerical and analytical approximations

The similarity solutions $w_{fa}(x,\bar{t})$ only provide reasonable approximations of the withdrawal process, if we find appropriate values of t_0 and also of A for the unbounded domain. As the initial condition (4.18) in general does not have the similarity shape and as vertical equilibrium conditions are only established some time after the start of the flow process, we estimate the unknown values from oil lens (shape) properties after a sufficiently large time, rather than from the initial condition. We compute t_0 and A from the numerical solutions for the free oil volume per unit lateral area w_{fn} of Section 4.1, where the subscript n identifies the numerical solution, by comparing w_{fn} with the analytical w_{fa} of Section 4.2. In practice, it is relatively easy to determine t_0 and A by measuring the outflow rate and by comparing it with the analytically obtained outflow rate. Measuring once yields the value of t_0 for the bounded domain, whereas measuring at two different times yields the values of both A and t_0 for the unbounded domain.

To obtain the values of A and t_0 from the numerical solution for $L=\infty$ (cases 3-10 of Table 1), we use at one time the moment M_{k-1} (4.31) and the oil outflow rate, $q(t)=\int_0^t\int_z u_o(0,\zeta,\tau)\,d\zeta\,d\tau$. Observe from Figure 6 that except for case 5 (large n) all cases with zero entrapment ($k=2$) had an approximately time-independent first moment in agreement with (4.21) after a short time. In case of entrapment (case 9 and 10) we computed $k=2.29$ and $k=2.48$ respectively and $M_{k-1,n}$ became time-independent as well. This indicates that, except for a large value of n (case 5), the flow processes quickly satisfied the vertical equilibrium conditions and that the boundary condition (4.16) was a good approximation of the non-reduced well condition. For the similarity solution we have

$$M_{k-1,a}=\nu^{-\frac{1}{2}k}\,A^{k+\frac{2}{m}}\,\tilde{M}_{k-1}, \tag{4.36}$$

where $\tilde{M}_{k-1}=\int\xi^{k-1}\,\tilde{h}\,d\xi$, the moment in terms of the transformed $\tilde{h}(\xi)$ (4.24), which is given by (4.35) for $k=2$ and obtained numerically for $k>2$. By identifying $M_{k-1,n}$ and $M_{k-1,a}$ at $t=0.1\,t_e$, we obtained the values of A, which are listed in Table 2.

The outflow rate is given for the similarity solution by

$$q_a(\bar{t})=-\gamma\,w_{fa}^m\,\frac{\partial\,w_{fa}}{\partial\,x}(0,\bar{t})=\gamma\,\nu^{\frac{1}{2}}\,\bar{t}^{-(m+1)\,\mu-\nu}\,A^{1+\frac{2}{m}}\,\tilde{y}(\xi=0), \tag{4.37}$$

with $\bar{t}=\gamma\,(t-t_0)$. For $p=1$ $\tilde{y}(\xi=0)$ is given by (4.34) and for $p>1$ it is computed numerically. We identify q_a and its numerical equivalent q_n at $t=0.1\,t_e$ and obtain the values of t_0, which are also

Table 2: Parameter values for the similarity solution and deviations of the analytical solution from the numerical solution

case	γ	A	t_0	Δv	case	γ	t_0	Δv
3	0.0680	1.68	-188	0.0305	11	0.0153	-207	0.0821
4	0.100	1.89	-63.3	-0.00766	12	0.0225	-83.6	0.114
5	0.0621	1.62	-1250	0.359	13	0.0140	-330	0.710
6	0.0170	1.41	-104	-0.0106	14	0.00764	-266	0.0127
7	0.215	1.74	-92.9	0.00794	15	0.0387	-101	0.0744
8	0.108	1.64	-92.1	0.0196	16	0.0244	-137	0.0225
9	0.0860	1.63	6.82	0.0269	17	0.0194	-168	0.105
10	0.0992	1.60	-30.1	0.0573	18	0.0223	-180	0.138

listed in Table 2.
The values of k, A and t_0 determine $w_{fa}(r,\bar{t})$. In Figure 8.a we present w_{fn} and w_{fa} for case 3 at several times. Observe that the agreement between the profiles is good, except near $x = 0$.

In Figure 8.b we present also the free oil volume v which is a global and practically relevant characteristic. The analytically and numerically obtained volumes show very good agreement at all times. For all cases (3-10) we calculated the relative deviations of v at the maximum computed time t_e

$$\Delta v = \frac{v_n(t_e) - v_a(t_e)}{v_n(t_e)}. \tag{4.38}$$

The values of Δv which are listed in Table 2, are less than 6 percent, except for large n.

When oil entrapment is taken into account (cases 9-10), the trapped oil volume per unit lateral area according to the analytical solution can be found in exactly the same way as described in [25].

For $L < \infty$ we obtain the value of t_0 by identifying the numerical oil outflow rate $q_n(t)$ at $x = 0$ and the outflow rate corresponding to the similarity solution, i.e.

$$q_a(\bar{t}) = -\gamma\, w_{fa}^m \frac{\partial\, w_{fa}}{\partial\, x}(0,\bar{t}) = \gamma\, \bar{t}^{-\frac{1}{m}-1}\, \tilde{y}(\xi = 0), \tag{4.39}$$

with $\tilde{y}(\xi = 0)$ given by (4.25), at $t = 0.1\, t_e$. In Figure 9 we present w_{fn} and w_{fa} for case 11 at several times and the free oil volumes v_n and v_a. The profiles show good agreement, except near $x = 0$ and the volumes agree very well at all times. For all cases (11-18) we computed also the deviations Δv (4.38), which are listed in Table 2. These deviations are less than 14 percent, except for large n (case 13). The deviations for the bounded domain are slightly larger than for the unbounded domain. This may be caused by numerical errors, as the absolute values of the remaining free oil volumes for the bounded domain became very small, see Figures 5.b and 9.b.

Although the approximation (4.16) of the well boundary condition, i.e. $w_f(0,t) = 0$, is not in agreement with the numerically obtained free oil volume per unit lateral area $w_{fn}(0,t)$, see Figures 8.a and 9.a, this approximation leads to almost correct outflow rates and thus to almost correct solutions. At the well boundary most oil is present above the oil seepage face, where no outflow occurs. This means that the largest fraction of $w_{fn}(0,t)$ does not contribute to the outflow rate. For large values of n (cases 5 and 13) as well as for small values of α (not shown here) the analytical approximations are less accurate and removal happens relatively slowly. For these parameter values the capillary pressure functions ($P_{ow}(S_{wa})$, $P_w(S_{wa})$ and $P_{ao}(S_t)$ of relations (2.4,2.5)) decrease rapidly from a relatively large value to zero, when the respective saturations approach one. This behavior corresponds to large entry pressures, which may explain that a larger fraction of $w_{fn}(0,t)$ contributes to the outflow rate and that the approximation (4.16) of the well boundary condition is less adequate.

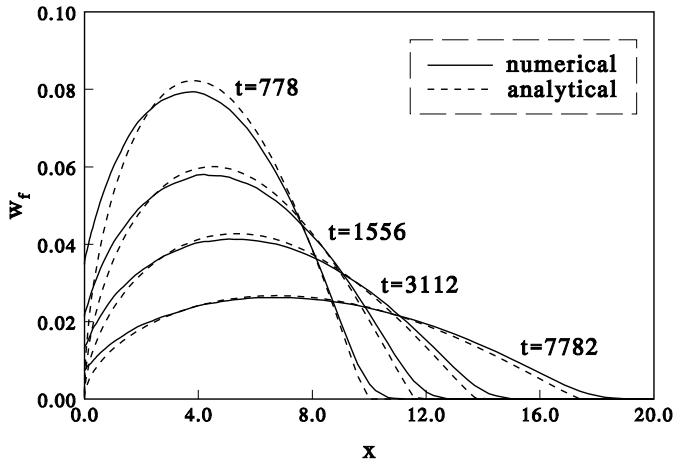

(a)

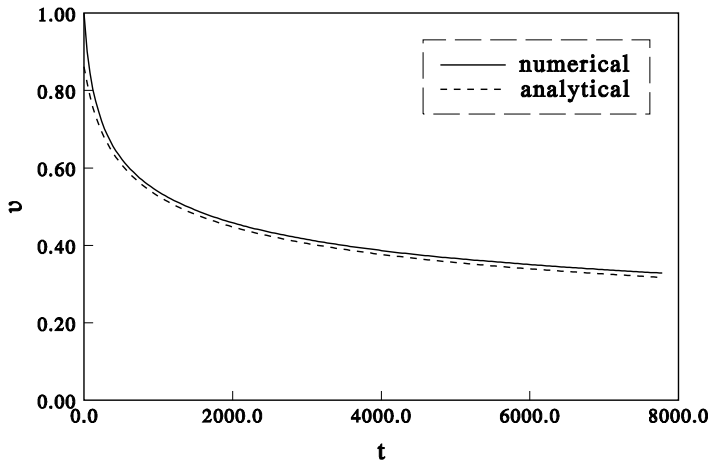

(b)

Figure 8: Numerical and analytical free oil volumes per unit lateral area (a) and free oil volumes in the domain (b) for case 3 after fitting parameters at $t = 778$.

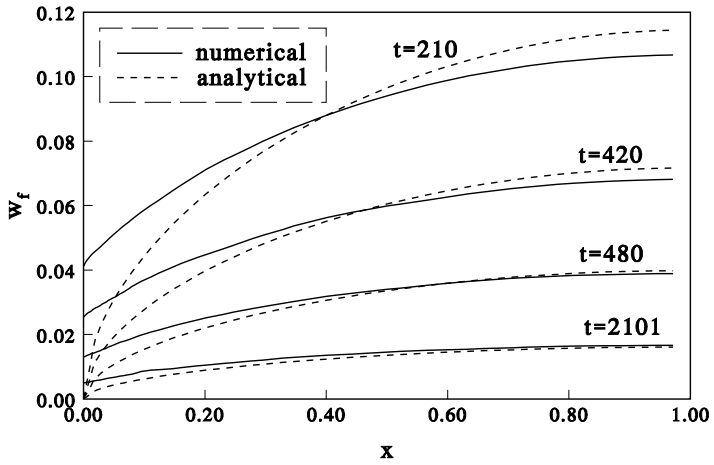

(a)

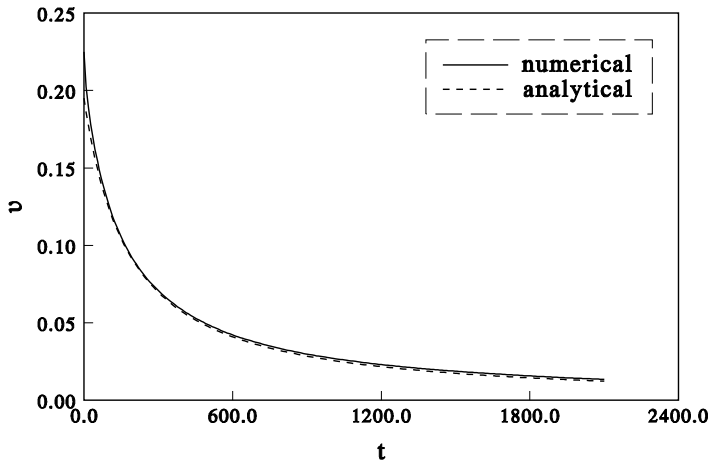

(b)

Figure 9: Numerical and analytical free oil volumes per unit lateral area (a) and free oil volumes in the domain (b) for case 11 after fitting parameters at $t = 210$.

5. Conclusions

We modeled withdrawal of a lens of organic contaminant in a two-dimensional domain, which is either finite or semi-infinite in the horizontal direction. At the well we imposed seepage face conditions for multi-phase flow, i.e. a phase can only flow out, in which case its pressure is equal to the pressure outside the soil.

Using a numerical multi-phase flow model we simulated the withdrawal process with a constant fluid level in the well that is equal to the phreatic surface in the soil. Implementation of the seepage face conditions as sink terms with a large artificial productivity index, as was proposed earlier, was compared with the direct implementation of the variational condition. For increasing values of the index the sink term solutions converged to the 'direct' solutions, but required much more computation time. Hence, the 'direct' implementation is both more accurate and more efficient. Close to the well boundary steep pressure gradients occurred. Refinement of the X-grid led to convergence of solutions near the seepage face. Oil outflow velocities showed a steep peak in vertical direction just below the top of the oil seepage face, which required very accurate discretization. Simulations for different parameters showed that removal was slower in the semi-infinite domain in which the oil lens continued to spread horizontally. For large values of the parameter n the removal rate was small. Even for the present simulations with no drawdown of the water table much oil became entrapped.

To derive analytical approximations we assumed vertical equilibrium of the oil lens and we integrated the oil flow equation vertically. We approximated the seepage face conditions by taking the oil volume per unit lateral area equal to zero, yielding however a nonzero outflow rate. Both for the bounded and the unbounded domain similarity solutions of the resulting differential equations were available, which were either explicit or easy to compute. For the unbounded domain a time-independent moment of the similarity solution was determined. The approximate independence of time of this moment for the corresponding numerical solution justified the vertical equilibrium assumption and the approximation of the well boundary condition. Comparison of the analytical and numerical moments for short times yielded the value of one of the unknown constants in the analytical solution. The remaining unknown constant was obtained by comparison of the numerically and analytically obtained outflow rates for the bounded and the unbounded domain. After fitting the two constants for a small time, the analytical solution was used to predict for larger times. Except for larger values of n, the agreement between analytical approximations and numerical results was good. In practice, the determination of the two constants in the analytical solution may be done using outflow rates, which are easily accesible, for two different times.

Appendix 1. Vertically integrated variables

The vertically integrated free oil saturation (4.5) is

$$w_f = \phi \int_{z_{ow}}^{z_u} (1 - S_{wa})\, dz - \phi \int_{z_{ao}}^{z_u} (1 - S_t)\, dz \tag{A 1}$$

We use the first two terms of the Taylor series expansion for small values of $\left(\frac{\alpha_{ow}\, P_{ow}}{\rho_w\, g}\right)^n$ and $\left(\frac{\alpha_{ao}\, P_{ao}}{\rho_w\, g}\right)^n$ in relations (2.4) and (2.5) and use relations (4.1) and (4.2) to approximate

$$1 - S_{wa} \sim (1 - \frac{1}{n})\,(\frac{\alpha_{ow}\, P_{ow}}{\rho_w\, g})^{\,n} = (1 - \frac{1}{n})\,(\frac{\rho_o}{\rho_w})^{\,n}\,(z_{ao} + \frac{\Delta\,\rho}{\rho_o}\, z)^{\,n} \tag{A 2}$$

$$1 - S_t \sim (1 - \frac{1}{n})\,(\frac{\alpha_{ao}\, P_{ao}}{\rho_w\, g})^{\,n} = (1 - \frac{1}{n})\,(\frac{\alpha_{ao}\, \rho_o}{\alpha_{ow}\, \rho_w})^{\,n}\,(z - z_{ao})^{\,n}. \tag{A 3}$$

Hence, we obtain

$$w_f \sim \delta_1\, z_{ao}^{n+1} \tag{A 4}$$

where

$$\delta_1 = \phi \, \frac{n-1}{n(n+1)} \, \frac{\rho_w}{\Delta \, \rho} \, \frac{1}{(1-D)^n}. \tag{A 5}$$

The vertically integrated relative permeability (4.6) is

$$\begin{aligned} \bar{k} &= \int_{z_{ow}}^{z_{ao}} (1 - S_{wa})^{\frac{1}{2}} \, (1 - S_{wa}^{\frac{n}{n-1}})^{2-\frac{2}{n}} \, dz + \\ &+ \int_{z_{ao}}^{z_u} (S_t - S_{wa})^{\frac{1}{2}} \, ((1 - S_{wa}^{\frac{n}{n-1}})^{1-\frac{1}{n}} - (1 - S_t^{\frac{n}{n-1}})^{1-\frac{1}{n}})^2 \, dz. \end{aligned} \tag{A 6}$$

We use again the Taylor series expansion to approximate

$$1 - S_{wa}^{\frac{n}{n-1}} \sim (\frac{\alpha_{ow} \, P_{ow}}{\rho_w \, g})^n = (\frac{\Delta \, \rho}{\rho_w})^n \, (z - z_{ow})^n \tag{A 7}$$

$$1 - S_t^{\frac{n}{n-1}} \sim (\frac{\alpha_{ao} \, P_{ao}}{\rho_w \, g})^n = (\frac{\alpha_{ao} \, \rho_o}{\alpha_{ow} \, \rho_w})^n \, (z - z_{ao})^n. \tag{A 8}$$

Only the first integral of equation (A 6), denoted by $\bar{k}_1$, can be approximated analytically, i.e.

$$\bar{k}_1 = \delta_2 \, z_{ao}^{\frac{5n}{2}-1}, \tag{A 9}$$

where

$$\delta_2 = \frac{2}{5n-2} \, (\frac{n-1}{n})^{\frac{1}{2}} \, \frac{\rho_w}{\Delta \, \rho}. \tag{A 10}$$

The second integral of equation (A 6), denoted by $\bar{k}_2$, is

$$\bar{k}_2 = I_k \, \delta_3 \, z_{ao}^{\frac{5n}{2}-1}, \tag{A 11}$$

where

$$\delta_3 = (\frac{n-1}{n})^{\frac{1}{2}} \, \frac{\rho_w}{\Delta \, \rho} \, \frac{D}{(1-D)^{\frac{5n}{2}-1}} \tag{A 12}$$

and the integral

$$I_k(n, D) = \int_0^1 ((D \, y + 1 - D)^n - y^n)^{\frac{1}{2}} ((D \, y + 1 - D)^{n-1} - y^{n-1})^2 \, dy, \tag{A 13}$$

that does not depend on z_{ao} and must be approximated numerically.

As a result we obtain

$$z_{ao} = \lambda_1 \, w_f^{\frac{1}{n+1}} \tag{A 14}$$

$$\bar{k} = \lambda_2 \, w_f^{\frac{5n-2}{2\,(n+1)}}, \tag{A 15}$$

where

$$\lambda_1 = \delta_1^{\frac{-1}{n+1}} = \phi^{\frac{-1}{n+1}} \, (\frac{n\,(n+1)}{n-1})^{\frac{1}{n+1}} \, (\frac{\Delta \, \rho}{\rho_w})^{\frac{1}{n+1}} \, (1-D)^{\frac{n}{n+1}} \tag{A 16}$$

$$\begin{aligned} \lambda_2 &= (\delta_2 + I_k \, \delta_3) \, \delta_1^{\frac{2-5n}{2\,(n+1)}} = \\ &= \phi^{\frac{2-5n}{2\,(n+1)}} \, (\frac{n-1}{n})^{\frac{3-4n}{2\,(n+1)}} \, (n+1)^{\frac{5n-2}{2\,(n+1)}} \, (\frac{\Delta \, \rho}{\rho_w})^{\frac{3n-4}{2\,(n+1)}} \, * \\ &\quad * (\frac{2}{5n-2} \, (1-D)^{\frac{n\,(5n-2)}{2\,(n+1)}} + \frac{D}{(1-D)^{\frac{5n-2}{2\,(n+1)}}} \, I_k). \end{aligned} \tag{A 17}$$

To obtain the the trapping constant c_t in (4.9), we introduce the additional elevations z_{ow}^{min}, z_{ao}^{max} and z_u^{max}, which determine the maximum oil and minimum water saturations. The trapped oil volume per unit lateral area is given by

$$\begin{aligned} w_t &= \theta\,\phi \int_{z_{ow}^{min}}^{z_u^{max}} (S_{wa} - S_w^{min})\,dz = \theta\,(\phi \int_{z_{ow}^{min}}^{z_u^{max}} (1 - S_w^{min})\,dz + \\ &- \phi \int_{z_{ow}}^{z_u} (1 - S_{wa})\,dz - \phi \int_{z_u}^{z_u^{max}} (1 - S_{wa})\,dz). \end{aligned} \tag{A 18}$$

Using (A 2) and (A 3) we obtain

$$\phi \int_{z_{ow}^{min}}^{z_u^{max}} (1 - S_w^{min})\,dz - \phi \int_{z_{ow}}^{z_u} (1 - S_{wa})\,dz \;\sim\; \frac{\delta_1}{1-D}\,((z_{ao}^{max})^{n+1} - z_{ao}^{n+1}). \tag{A 19}$$

For $z_u < z < z_u^{max}$ S_{wa} is given by the third expression of (2.4), therefore we approximate

$$\phi \int_{z_u}^{z_u^{max}} (1 - S_{wa})\,dz \sim \phi\,\frac{n-1}{n(n+1)}\,\frac{\beta_{ow}}{(1-D)^{n+1}}\,((z_{ao}^{max})^{n+1} - z_{ao}^{n+1}). \tag{A 20}$$

Hence, we combine (A 19) and (A 20) to obtain

$$w_t = \delta_1\,\theta\,\frac{\rho_o}{\rho_w}\,((z_{ao}^{max})^{n+1} - z_{ao}^{n+1}) = \theta\,\frac{\rho_o}{\rho_w}\,(w_m - w_f), \tag{A 21}$$

yielding $c_t = \theta\,\dfrac{\rho_o}{\rho_w}$.

Appendix 2. Evaluation of the ordinary differential equation

For the scaled variable $\tilde{h}(\xi)$ we solve the nonlinear differential equation

$$(\tilde{h}^m\,\tilde{h}\,')' = F(-\xi\,\tilde{h}\,' - k\,\tilde{h}) \quad \text{for } 0 < \xi < 1, \tag{A 1}$$

with boundary conditions

$$\tilde{h}(0) = 0, \quad \tilde{h}(1) = 0. \tag{A 2}$$

Furthermore, in view of condition (4.20) we impose

$$\tilde{h}^{m-1}\,\tilde{h}\,'(1) = -p. \tag{A 3}$$

Therefore, on the right half of the domain we transform equation (A 1) into a system of two differential equations with

$$y_{r,1} = \tilde{h}^m \quad \text{and} \quad y_{r,2} = \tilde{h}^{m-1}\,\tilde{h}\,'. \tag{A 4}$$

This yields

$$\begin{cases} y_{r,1}' &= m\,y_{r,2} \\ y_{r,2}' &= -\dfrac{y_{r,2}^2}{y_{r,1}} + F(-\xi\,\dfrac{y_{r,2}}{y_{r,1}} - k) \end{cases} \qquad \text{for } \frac{1}{2} < \xi < 1, \tag{A 5}$$

with boundary conditions $y_{r,1}(1) = 0$ and $y_{r,2} = -p$.

Since near $\xi = 0$ the flux $\tilde{h}^m \tilde{h}'$ is nonzero and bounded, on the left half of the domain we transform equation (A 1) into a system of two differential equations with

$$y_{l,1} = \tilde{h}^{m+1} \quad \text{and} \quad y_{l,2} = \tilde{h}^m \tilde{h}'. \tag{A 6}$$

This yields

$$\begin{cases} y'_{l,1} &= (m+1)\, y_{l,2} \\ y'_{l,2} &= F(-\xi \dfrac{y_{l,2}}{y_{l,1}^{\frac{m}{m+1}}} - k\, y_{l,1}^{\frac{1}{m+1}}) \end{cases} \qquad \text{for } 0 < \xi < \frac{1}{2}, \tag{A 7}$$

with boundary condition $y_{l,1}(0) = 0$.

Imposing continuity of $\tilde{h}$ and $\tilde{h}'$ at $\xi = \dfrac{1}{2}$, the two systems (A 5) and (A 7) are solved sequentially by shooting backward from $\xi = 1$ using a fourth order Runge-Kutta scheme. As $y_{l,1}(0)$ varies monotonically with k we can use a simple iteration to vary k untill the solution satisfies $y_{l,1}(0) = 0$.

Appendix 3. Removal in a three-dimensional domain

Removal of oil through a horizontal ditch in a three-dimensional semi-infinite domain under vertical flow equilibrium conditions is described similar to equation (4.11) by

$$F\,(\frac{\partial\, w_f}{\partial\, t}) = \gamma\, \nabla\, \cdot\, (w_f^m\, \nabla\, w_f) \quad \text{for} \quad t > 0,\ 0 < x_1 < \infty,\ 0 < x_2 < f(x_1, t) \tag{A 1}$$

where the ditch is located at $x_1 = 0$. The curve $x_2 = f(x_1, t)$ defines the free boundary beyond which no oil is present and we assume that f is finite for all values of $x_1 \geq 0$ and $t > 0$. Similar to (4.16) and (4.18) we impose

$$w_f\,(0, x_2, t) = 0 \tag{A 2}$$

and

$$w_f\,(x_1, x_2, 0) = w_i(x_1, x_2), \tag{A 3}$$

with

$$\int_0^\infty \int_0^f w_i(x_1, x_2)\, dx_2\, dx_1 = 1, \tag{A 4}$$

the prescribed inital volume. Furthermore, we impose by symmetry

$$\frac{\partial\, w_f}{\partial\, x_2}(x_1, 0, t) = 0. \tag{A 5}$$

In analogy to (4.28) equation (A 1) admits a similarity solution of the form [15]

$$w_{f\,a}\,(x_1, x_2, t) = t^{-\mu} h(\vec{\eta}), \quad \vec{\eta} = \begin{pmatrix} \eta_1 \\ \eta_2 \end{pmatrix} = \nu^{\frac{1}{2}} t^{-\nu} \begin{pmatrix} x_1 \\ x_2 \end{pmatrix}, \tag{A 6}$$

with constants μ and ν satisfying (4.30), which is positive for $0 < \eta_1 < a$ and $0 \leq \eta_2 < g(\eta_1)$ with $a = g(0)$. The set $\Gamma = \{0 \leq \eta_1 \leq a, \eta_2 = g(\eta_1)\}$ denotes the free boundary for the similarity solution. Substitution of (A 6) into equation (A 1) yields

$$\nabla \cdot (h^{\,m} \nabla h) + \vec{\eta} \cdot \nabla h + k\, h = 0 \quad \text{for } 0 < \eta_1 < a,\ 0 < \eta_2 < g(\eta_1), \tag{A 7}$$

with $k = \dfrac{\mu}{\nu}$. Imposing the transformed versions of conditions (A 2) and (A 4), i.e.

$$h(\vec{\eta})|_{\eta_1=0} = 0 \quad \text{and} \quad \frac{\partial h}{\partial \eta_2}(\vec{\eta})|_{\eta_2=0} = 0, \tag{A 8}$$

requires $k \geq 3$, whereas $k = 3$ for $p = 1$ (no trapping). Similar to property (A 3) we have

$$(h^{\,m-1}\nabla h + \vec{\eta}) \cdot \nabla h = 0 \quad \text{for} \quad \vec{\eta} \in \Gamma. \tag{A 9}$$

Since h is also invariant under a scaling similar to (4.24), it is possible to solve for this similarity solution in two dimensions and to obtain an analytical approximation of light oil removal in a three-dimensional situation.

Acknowledgement
This project was partly funded by the Netherlands Organization for Scientific Research (NWO project NLS 61-251).

References

1. Aziz, K. & Settari, A., *Petroleum reservoir simulation*, Academic Press, New York, 1979.
2. Baiocchi, C. & Capelo, A., *Variational and quasivariational inequalities*, John Wiley, New York, 1984.
3. Barenblatt, G.I., *Dimensional analysis*, Gordon and Breach, New York, 1987.
4. Barenblatt, G.I., Entov, V.M. & Ryzhik, V.M., *Theory of fluid flows through natural rocks*, Kluwer Academic Publishers, Dordrecht, 1990.
5. Barenblatt, G.I. & Zel'dovich Y.B., On dipole-solutions in problems of nonstationary filtration of gas under polytropic regime, Prikl. Mat. Mekh. 21 (1957) 718-720.
6. Bear, J., *Dynamics of fluids in porous media*, Elsevier, New York, 1972.
7. Bear, J., Ryzhik, V., Braester, C. & Entov, V., On the movement of an LNAPL lens on the water table, Transport in Porous Media 25 (1996) 283-311.
8. Blunt, M., Dengen Z. & Fenwick, D., Three phase flow and gravity drainage in porous media, Transport in Porous Media 20 (1995) 77-103.
9. Celia, M.A., Bouloutas, E.T. & Zarba, R.L., A general mass-conservative numerical solution for the unsaturated flow equation, Water Resour. Res. 26 (1990) 1483-1496.
10. Chavent, G. & Jaffré, J., *Mathematical models and finite elements for reservoir simulation*, ed. J.L. Lions, Studies in mathematics and its applications, Vol 17, North-Holland, Amsterdam, 1986.
11. Corapcioglu, M.Y., Tuncay, K., Lingam, R. & Kambham, K.K.R., Analytical expressions to estimate the free product recovery in oil-contaminated aquifers, Water Resour. Res. 30 (1994) 3301-3311.
12. Crank, J., *Free and moving boundary problems*, Clarendon Press, Oxford, 1984.
13. Dake, L.P., *Fundamentals of reservoir engineering*, Elsevier, Amsterdam, 1978.
14. Duvaut, G. & Lions, J.L., *Inequalities in mechanics and physics*, Springer, Berlin, 1976.
15. Hulshof, J. & Vazquez, J.L., The dipole solution for the porous medium equation in several space dimensions, Ann. d. Scu. Norm. Sup. d. Pisa, Serie IV, 20 (1993), 193-217.
16. Huyakorn, P.S., Wu, Y.S. & Park, N.S., An improved sharp-interface model for assessing NAPL contamination and remediation of groundwater systems, J. Contam. Hydrol. 16 (1994) 203-234.
17. Kaluarachchi, J.J. & Parker, J.C., Multiphase flow with a simplified model for oil entrapment, Transport in Porous Media 7 (1992) 1-14.

18. Land, C.S., Calculation of imbibition relative permeability for two- and three-phase flow from rock properties, Trans. Am. Inst. Min. Metall. Pet. Eng. 243 (1968) 149-156.

19. Lenhard, R.J. & Parker, J.C., A model for hysteretic constitutive relations governing multiphase flow, 2. permeability-saturation relations, Water Resour. Res. 23 (1987) 2197-2206.

20. Lenhard, R.J. & Parker, J.C., Estimation of free hydrocarbon volume from fluid levels in monitoring wells, Ground Water 28 (1990) 57-67.

21. Miller, C.A. & Van Duijn, C.J., Similarity solutions for gravity-dominated spreading of a lens of organic contaminant, Environmental studies: mathematical, computational and statistical analysis, ed. M.F. Wheeler. IMA Volumes in Mathematics and its Applications, Vol. 79, Springer-Verlag, New York, 1995.

22. Parker, J.C. & Lenhard, R.J., A model for hysteretic constitutive relations governing multiphase flow, 1. saturation-pressure relations, Water Resour. Res. 23 (1987) 2187-2196.

23. Parker, J.C. & Lenhard, R.J., Vertical integration of three-phase flow equations for analysis of light hydrocarbon plume movement, Transport in Porous Media 5 (1989) 187-206.

24. Van Dijke, M.I.J., Van der Zee, S.E.A.T.M. & Van Duijn, C.J., Multi-phase flow modeling of air sparging, Adv. Water Resour 18 (1995) 319-333.

25. Van Dijke, M.I.J. & Van der Zee, S.E.A.T.M., A similarity solution for oil lens redistribution including capillary forces and entrapment, Transport in Porous Media (1997) in press.

26. Wu, Y.-S., Huyakorn, P.S. & Park, N.S., A vertical equilibrium model for assessing nonaqueous phase liquid contamination and remediation of groundwater systems, Water Resour. Res. 30 (1994) 903-912.

27. Wu, Y.-S., Forsyth, P.A. & Jiang, H., A consistent approach for applying numerical boundary conditions for multiphase subsurface flow, J. Contamin. Hydrology 23 (1996) 157-184.

28. Yortsos, Y.C., A theoretical analysis of vertical flow equilibrium, Transport in Porous Media 18 (1995) 107-129.